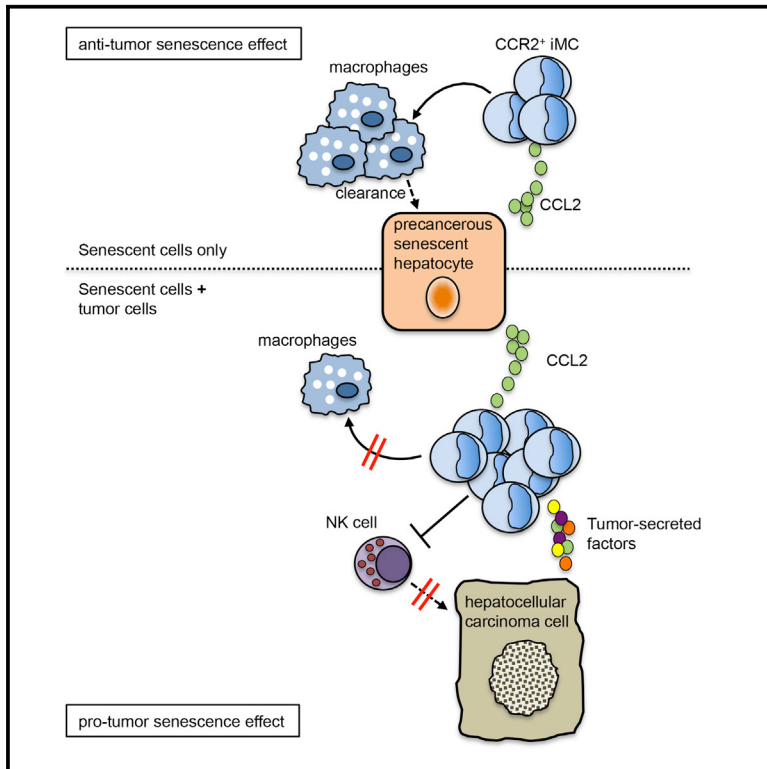


Distinct Functions of Senescence-Associated Immune Responses in Liver Tumor Surveillance and Tumor Progression

Graphical Abstract



Authors

Tobias Eggert, Katharina Wolter, Juling Ji, ..., Xin Wei Wang, Lars Zender, Tim F. Greten

Correspondence

lars.zender@med.uni-tuebingen.de (L.Z.), tim.greten@nih.gov (T.F.G.)

In Brief

Eggert et al. show that CCL2 is secreted from oncogene-induced senescent hepatocytes to recruit CCR2⁺ immature myeloid cells (iMC). These iMC differentiate into macrophages that clear pre-malignant senescent cells, but iMC promote growth of established hepatocellular carcinoma through NK cell inhibition.

Highlights

- The CCL2-CCR2 axis is necessary for clearance of pre-cancerous senescent hepatocytes
- Absence of the CCL2-CCR2 axis leads to HCC outgrowth from senescent hepatocytes
- Peritumoral tissue senescence accelerates growth of HCC in mice and humans
- Senescence-recruited CCR2⁺ myeloid cells enhance HCC growth by NK cell inhibition



Distinct Functions of Senescence-Associated Immune Responses in Liver Tumor Surveillance and Tumor Progression

Tobias Eggert,¹ Katharina Wolter,² Juling Ji,³ Chi Ma,¹ Tetyana Yevsa,² Sabrina Klotz,² José Medina-Echeverz,¹ Thomas Longerich,⁴ Marshonna Forgues,³ Florian Reisinger,^{5,6} Mathias Heikenwalder,^{5,6} Xin Wei Wang,³ Lars Zender,^{2,7,*} and Tim F. Greten^{1,8,*}

¹Gastrointestinal Malignancy Section, Thoracic and Gastrointestinal Oncology Branch, Center for Cancer Research, National Cancer Institute, National Institutes of Health, Bethesda, MD 20892, USA

²Division of Gastrointestinal Oncology, Department of Internal Medicine I, University of Tübingen, 72076 Tübingen, Germany

³Laboratory of Human Carcinogenesis, Center for Cancer Research, National Cancer Institute, National Institutes of Health, Bethesda, MD 20892, USA

⁴Institute of Pathology, University Hospital RWTH Aachen, 52074 Aachen, Germany

⁵Institute of Virology, Technische Universität München and Helmholtz Zentrum München, 81675 Munich, Germany

⁶Division of Chronic Inflammation and Cancer, German Cancer Research Center (DKFZ), 69120 Heidelberg, Germany

⁷Translational Gastrointestinal Oncology Group within the German Consortium for Translational Cancer Research (DKTK), German Cancer Research Center (DKFZ), 69120 Heidelberg, Germany

⁸Lead Contact

*Correspondence: lars.zender@med.uni-tuebingen.de (L.Z.), tim.greten@nih.gov (T.F.G.)

<http://dx.doi.org/10.1016/j.ccell.2016.09.003>

SUMMARY

Oncogene-induced senescence causes hepatocytes to secrete cytokines, which induce their immune-mediated clearance to prevent tumor initiation, a process termed “senescence surveillance.” However, senescent hepatocytes give rise to hepatocellular carcinomas (HCCs), if the senescence program is bypassed or if senescent cells are not cleared. Here, we show context-specific roles for CCR2⁺ myeloid cells in liver cancer. Senescence surveillance requires the recruitment and maturation of CCR2⁺ myeloid cells, and CCR2 ablation caused outgrowth of HCC. In contrast, HCC cells block the maturation of recruited myeloid precursors, which, through NK cell inhibition, promote growth of murine HCC and worsen the prognosis and survival of human HCC patients. Thus, while senescent hepatocyte-secreted chemokines suppress liver cancer initiation, they may accelerate the growth of fully established HCC.

INTRODUCTION

Cellular senescence is a stress-response program, which induces a proliferative arrest in cells at risk of malignant transformation and is therefore widely considered to be an anti-tumor mechanism (Kuilman et al., 2010). In addition to this cell-autonomous mechanism of cancer prevention, senescent cells can secrete different cytokines including interleukin-1 (IL-1) and IL-6 (senescence-associated secretory phenotype [SASP]), which affect

neighboring tissue and immune cells (Acosta et al., 2013; Coppe et al., 2010; Kuilman et al., 2008). Recent research has shown that SASP factors can trigger senescence in an autocrine or paracrine fashion and thereby enhance the anti-tumor effect (Acosta et al., 2013; Kuilman et al., 2008). Paradoxically, depending on the context, the SASP can also have pro-tumor effects on neighboring cells by inducing proliferation via cytokines and growth factors (Jackson et al., 2012; Krtolica et al., 2001; Kuilman et al., 2010).

Significance

HCC constitutes the second most common cause of cancer-related death worldwide, and myeloid cells have been shown to play critical roles in HCC development. Here, we show that senescence-induced CCL2-CCR2 signaling and the ensuing myeloid cell accumulation harbor context-dependent functions in preventing HCC initiation, but also in promoting progression of established HCC. These findings have important implications for further clinical development of CCR2 antagonists, which are being evaluated for the treatment of various diseases. CCR2 antagonists may reduce tumor-induced immunosuppression in patients with advanced HCC but may fuel liver cancer growth in patients with chronic liver disease.

In the liver, cellular senescence has been linked to hepatocellular carcinoma (HCC) suppression (Kang et al., 2011; Lujambio et al., 2013). Senescent hepatocytes are different from wild-type hepatocytes, which are also mostly cell-cycle arrested, due to particular SASP-inducing chromatin changes (Kuilman et al., 2010). A hallmark of the cellular senescence program is also the induction of anti-proliferative proteins, such as p21 and p53. One senescence-inducing stressor in the liver is chronic inflammation, leading to repetitive waves of hepatocyte death, compensatory regeneration of hepatocytes, and either replicative senescence or oncogene-induced senescence upon the aberrant activation of oncogenes. Importantly, abrogation of oncogene-induced senescence leads to aggressive HCC development (Kang et al., 2011; Mudbhary et al., 2014).

Senescent hepatocytes via their SASP can recruit and activate immune cells, which clear senescent hepatocytes (termed “senescence surveillance”) and thereby prevent malignant transformation (Kang et al., 2011). In line with the postulation of cellular senescence as a cancer-protective mechanism is the finding that the abrogation of the senescence program due to additional oncogenic mutations, e.g., p53 mutation, causes aggressive HCC development (Mudbhary et al., 2014), but restoration of p53 in liver tumors can trigger immune cell-mediated clearance of senescent tumor cells (Iannello et al., 2013; Xue et al., 2007).

One key factor secreted by senescent cells, in particular senescent pre-cancerous hepatocytes, is CCL2, also known as MCP-1 (Kang et al., 2011). Senescent cells accumulate in chronically damaged livers (Jurk et al., 2014), in which HCCs commonly develop. Thus, cells undergoing oncogenic transformation, readily established tumor cells, and senescent hepatocytes co-exist in HCC-bearing livers (Mudbhary et al., 2014). However, the potential effect of CCL2 secreted by senescent hepatocytes on neighboring non-senescent tumor cells has not been investigated. Thus, we set out to characterize the role of CCL2-CCR2 signaling in early stages of liver tumor development and later stages of liver tumor progression by employing a model of oncogene-induced hepatocyte senescence.

RESULTS

CCL2-CCR2 Signaling Mediates Myeloid Cell Accumulation in Senescent Livers

Nras^{G12V} has been reported to trigger oncogene-induced senescence in mouse livers, and the chemokine CCL2 (MCP-1) was among the factors found to be secreted by senescent hepatocytes (Kang et al., 2011). Furthermore, senescence-recruited immune cells cleared pre-cancerous senescent hepatocytes. To functionally characterize the significance of CCL2-CCR2 for immune surveillance of pre-cancerous senescent cells, we stably delivered transposable elements encoding oncogenic *Nras*^{G12V} or an *Nras*^{G12V} effector loop mutant incapable of signaling to downstream pathways (*Nras*^{G12V/D38A}, hereafter referred to as *Nras*^{D38A}) into either wild-type or CCR2 knockout (KO) mouse livers (Figure 1A); accordingly, only *Nras*^{G12V} causes oncogene-induced senescence in livers (hereafter referred to as senescent livers), while *Nras*^{D38A} does not (hereafter referred to as non-senescent livers).

Nras^{G12V}- or *Nras*^{D38A}-expressing hepatocytes were purified from mouse livers after hydrodynamic delivery, and cytokine profiling was conducted on cell-culture supernatants of isolated hepatocytes (Figures S1A and S1B). As reported, several chemokines, including CCL2, were induced in senescent hepatocytes (*Nras*^{G12V}) compared with non-senescent (*Nras*^{D38A}) hepatocytes. We next studied the intrahepatic accumulation of CCR2-expressing immune cells in senescent livers. Flow cytometry analysis of CCR2-expressing hepatic immune cell infiltrates revealed that in *Nras*^{G12V}-injected livers myeloid cells constituted the vast majority of CCR2-expressing liver-infiltrating immune cells, with immature myeloid cells (iMC, CD11b⁺Gr-1⁺) and macrophages (CD11b⁺F4/80⁺Gr-1⁻) being the main contributors to the CCR2⁺ immune cell population (Figures 1B and S2A). iMC can be further subdivided based on their surface molecule expression into granulocytic (CD11b⁺Gr-1^{high}Ly6C^{low}) or monocytic iMC (CD11b⁺Gr-1^{low}Ly6C^{high}) (Figures 1B–1D and S2A–S2C). After *Nras*^{G12V} delivery, the number of CCR2⁺ iMC and CCR2⁺ macrophages significantly increased compared with *Nras*^{D38A}-injected mice (Figures 1C and 1D), suggesting that signaling through the CCL2 receptor, CCR2, leads to a senescence-mediated expansion of iMC and macrophages in the liver.

We next analyzed the levels of myeloid cells in livers of CCR2 KO mice (Figures 1E, 1F, S2C, and S2D). In line with the hypothesis that CCR2 deficiency would impair homing of monocytes to mouse livers harboring senescent hepatocytes, we found markedly reduced monocytic iMC numbers in CCR2 KO mouse livers compared with wild-type mouse livers after stable *Nras*^{G12V} delivery (Figure 1E). In support of the concept that monocytes differentiate into macrophages after homing to the mouse liver (Kang et al., 2011), we also found strongly reduced macrophage numbers in CCR2 KO mouse livers compared with wild-type mouse livers after hydrodynamic delivery of *Nras*^{G12V} (Figure 1E). Moreover, we found an *Nras*^{G12V}-dependent expansion of other CCR2⁺ immune cells, including lymphocytes (Figure S2A). However, only monocytic iMC and macrophages homogeneously express CCR2, while CCR2 expression on other immune cells is limited to subfractions of cells (Figure S2B). Consequently, *Nras*^{G12V} delivery into CCR2 KO mice specifically led to significantly fewer monocytic iMC and macrophages in the liver (Figure S2C). Senescence-induced myeloid cell and macrophage accumulation in wild-type mouse livers and an absence of such an increase in CCR2 KO mice was additionally confirmed by immunohistochemistry staining for CD11b and MHC-II (Figures S3A and S3B). Furthermore, experiments in senescence-deficient p19 KO mice revealed that cytokine expression and subsequent myeloid cell accumulation in *Nras*^{G12V}-expressing livers depend on cellular senescence (Figures S1B, S3A, and S3B).

To rule out potential effects of non-immune cell CCR2 deficiency in CCR2 KO mice on senescence-induced myeloid cell accumulation, we generated bone marrow chimeric mice to restrict CCR2 ablation to the hematopoietic compartment and compared the *Nras*^{G12V}-induced accumulation of monocytic iMC and macrophages side by side with wild-type and CCR2 full-body KO mice (Figure 1F). Reduced hepatic accumulation of these cells not only in CCR2 full-body KO, but also in bone marrow chimeric mice (CCR2 KO→WT) confirmed that senescence-induced hepatic myeloid cell accumulation is mediated

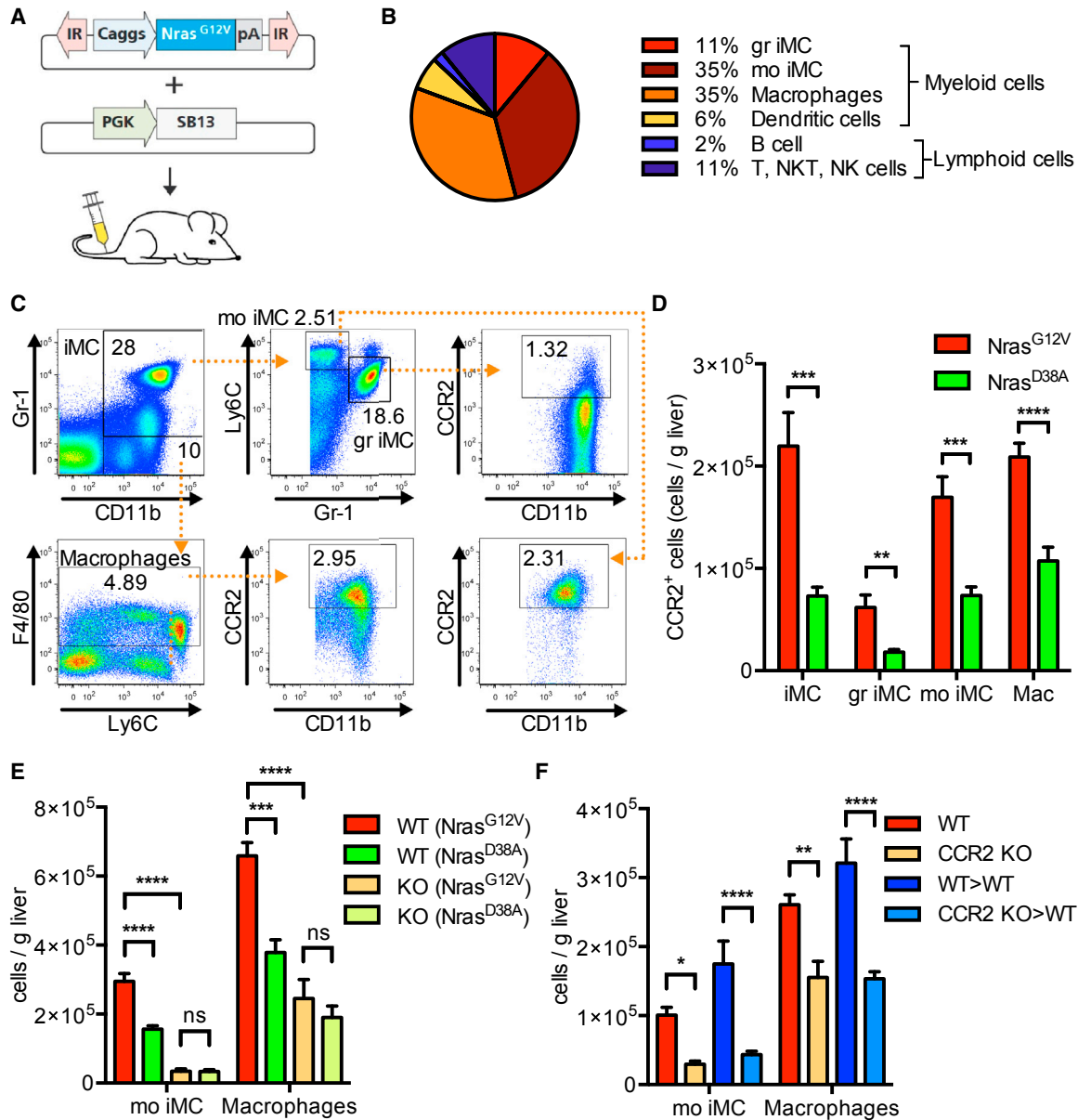


Figure 1. The CCL2-CCR2 Axis Mediates Myeloid Cell Accumulation in Senescent Livers

(A) Schematic representation of cellular senescence induction in mouse livers.

(B) CCR2⁺ hepatic immune cells (*Nras*^{G12V}). Distribution of CCR2-expressing immune cell subsets among liver-infiltrating immune cells in *Nras*^{G12V}-injected mice analyzed by flow cytometry.

(C and D) Quantification of CCR2⁺ myeloid cell subsets by flow cytometry 6 days after delivery of indicated genes in livers of C57BL/6 mice. iMC, immature myeloid cells; gr iMC, granulocytic iMC; mo iMC, monocytic iMC; Mac, macrophages. (C) Representative dot plots and gating of monocytic and granulocytic iMC and macrophages. Numbers within dot plots indicate frequency of gated cells among live cells. (D) The total cell number per gram of liver tissue of CCR2⁺ myeloid cell subsets 6 days after delivery of indicated genes.

(E) Quantification of the total cell number of mo iMC and macrophages by flow cytometry 5 days after delivery of indicated genes in livers of C57BL/6 or CCR2 KO mice. WT, wild-type.

(F) Quantification of the total cell number of hepatic mo iMC and macrophages by flow cytometry 5 days after hydrodynamic delivery of *Nras*^{G12V} into C57BL/6, CCR2 KO mice and WT → WT and CCR2 KO → WT chimeric mice. WT, wild-type.

Values are mean ± SEM; *p ≤ 0.05, **p ≤ 0.01, ***p ≤ 0.001, ****p ≤ 0.0001; ns, not statistically significant. Student's t test was used in (D) and two-way ANOVA in (E) and (F) to calculate statistical significance. Each experiment was performed two or three times with n ≥ 6 mice per group. See also [Figures S1](#) and [S2](#).

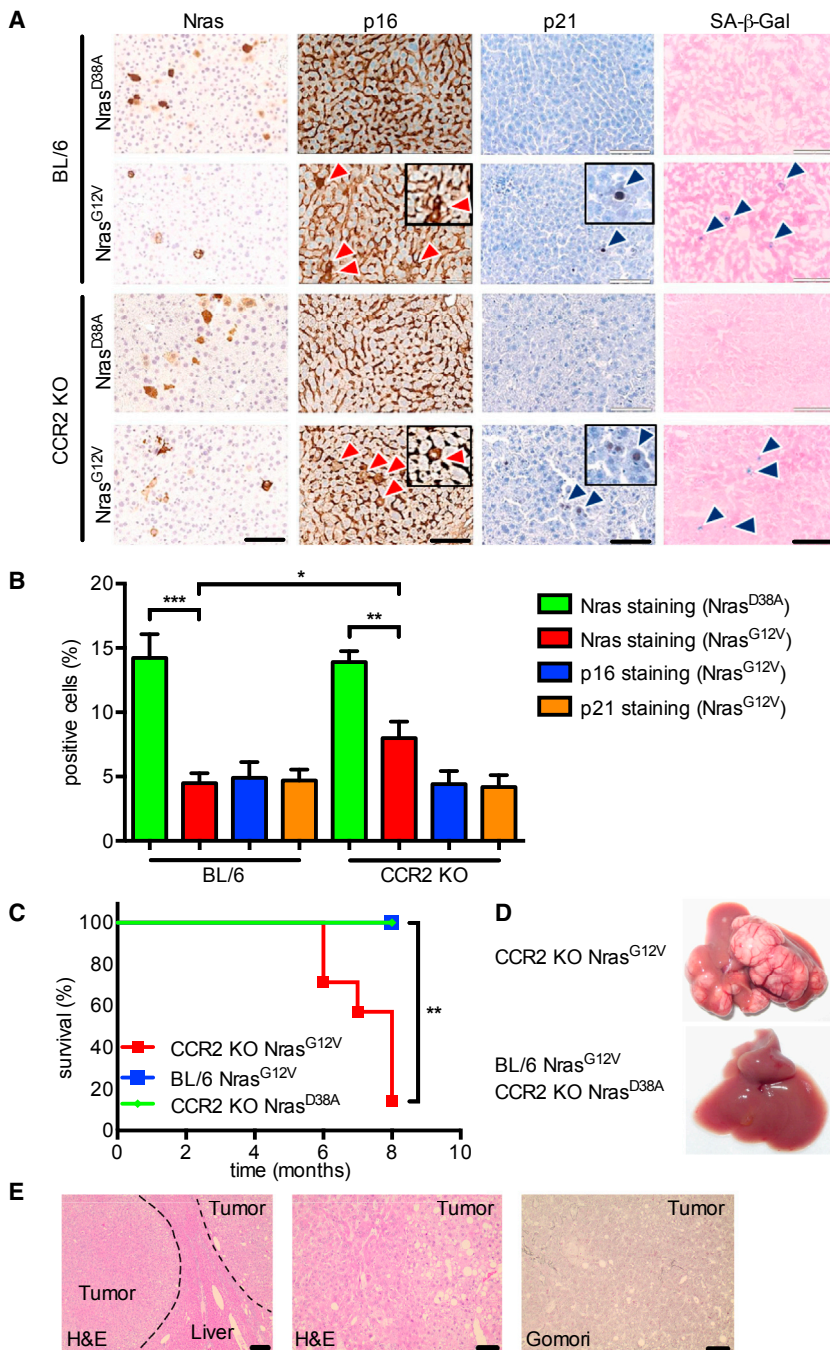


Figure 2. “Senescence Surveillance” Is Inhibited in CCR2 KO Mice and Results in Development of Aggressive HCCs

(A and B) Quantification (B) of Nras-, p16-, p21-, and SA-β-Gal-positive cells 12 days after intrahepatic delivery of *Nras*^{G12V} or *Nras*^{D38A} on liver sections from C57BL/6 wild-type or CCR2 KO mice, with (A) showing representative liver sections. Arrowheads in (A) indicate positive staining. Scale bars, 100 μm.

(C) Kaplan-Meier survival curve of C57BL/6 wild-type or CCR2 KO mice after *Nras*^{G12V} (both strains) or *Nras*^{D38A} (CCR2 KO only) delivery.

(D) Representative macroscopic images of livers from C57BL/6 wild-type or CCR2 KO mice 7 months after *Nras*^{G12V} (both strains) or *Nras*^{D38A} (CCR2 KO only) delivery.

(E) H&E staining (left: 1 × 40; scale bar, 200 μm; middle: 1 × 100; scale bar, 100 μm) and Gomori staining (right: 1 × 100; scale bar, 100 μm) of liver tumors isolated from a CCR2 KO mouse 6 months after stable intrahepatic delivery of oncogenic *Nras*^{G12V} via transposable elements. Explanted liver tumors were diagnosed as multinodular HCC (G2) with nodule-in-nodule growth and steatohepatic features; focal dense portal lymphoid infiltrates suggestive of incipient lymphoma.

Each experiment was performed two times with n = 4–6 mice per group. Values are mean ± SEM; *p ≤ 0.05, **p ≤ 0.01, ***p ≤ 0.001. Student’s t test was used in (B) to calculate statistical significance. See also Figure S3.

senescent hepatocytes can result, after an escape from the senescence program, in the outgrowth of HCC (Kang et al., 2011). Therefore, we next set out to study whether impaired monocyte and macrophage accumulation in senescent livers due to absence of CCR2 would have a similar effect. To this end, we quantified numbers of Nras-expressing hepatocytes (*Nras*^{G12V} or effector loop mutant *Nras*^{D38A}) and senescent hepatocytes (as determined by the senescence markers p16 and p21) in wild-type as well as CCR2 KO livers. We found equal numbers of *Nras*^{G12V}-expressing cells and p21-expressing senescent cells in wild-type mice, suggesting that every *Nras*^{G12V}-expressing hepatocyte enters

by hematopoietic CCR2. Together, these data suggest that senescent hepatocytes recruit iMC and macrophages through CCL2-CCR2 signaling.

Senescence-Associated CCL2-CCR2 Signaling Acts as Tumor Suppressive in Early Stages of Liver Tumorigenesis

Depletion of monocytes or macrophages via anti-Gr-1 antibody or gadolinium, respectively, has been shown to impair the clearance of senescent cells. Importantly, an impaired clearance of

a cellular senescence arrest (Figures 2A, 2B, and S3C). Compared with *Nras*^{D38A} effector loop mutant-expressing mouse livers, we found significantly fewer Nras-positive cells in *Nras*^{G12V}-expressing mouse livers, suggesting that at the investigated time point (12 days after stable intrahepatic transposon delivery) many of these cells already had been cleared by the immune system (Figures 2A and 2B). Interestingly, when we analyzed CCR2 KO mouse livers after hydrodynamic delivery of the same *Nras*^{G12V} and *Nras*^{D38A} transposon vectors, we found higher overall numbers of Nras-positive cells compared

with wild-type livers, indicating impaired senescent cell clearance. However, we also found that in CCR2 KO livers only about 65% of *Nras*^{G12V}-expressing cells stained positive for the senescence markers p16 and/or p21 (Figures 2A and 2B), suggesting compromised senescence induction. Based on these data, we hypothesized that CCR2 deficiency might affect senescence surveillance by three mechanisms: (1) due to absent infiltration of CCR2⁺ monocytes and macrophages into senescent mouse livers, there is less immune clearance of pre-cancerous senescent hepatocytes; (2) due to the lack of CCR2 on hepatocytes there is a less efficient senescence induction and enforcement, a finding which would follow a recent report showing that the non-related chemokine receptor CXCR2 (IL8RB) is crucial for senescence induction and reinforcement (Acosta et al., 2008); and (3) the reduced number of infiltrating monocytes and macrophages in CCR2 KO livers may result in decreased levels of cytokines and other factors derived from these immune cells, which play a role in senescence induction or reinforcement, thus resulting in *Nras*^{G12V}-expressing cells, which do not undergo senescence. To distinguish between these possibilities, we stably delivered transposable elements encoding *Nras*^{G12V} and CCR2-shRNAs into murine hepatocytes *in vivo*, thus generating CCR2 deficiency restricted to *Nras*^{G12V}-expressing hepatocytes (Figures S3D and S3E). Quantification of *Nras*-positive hepatocytes at 9 days after transposon delivery revealed equal numbers in mice where CCR2-small hairpin RNAs (shRNAs) were co-expressed with *Nras*^{G12V} and mice where a control shRNA was co-expressed. Therefore, hepatocyte-specific CCR2 deficiency does not affect the clearance of *Nras*^{G12V}-expressing hepatocytes, and hepatocytic CCR2 is not crucial for senescence induction or reinforcement. However, a reduced infiltration of senescent livers by CCR2⁺ monocytic iMC and CCR2⁺ macrophages (Figure 1) results in persistence of *Nras*-positive cells, which in part may be attributed to an impaired senescence induction/reinforcement due to a lack of immune cell-secreted factors.

Both an impaired clearance of senescent pre-cancerous hepatocytes and impaired senescence induction upon *Nras*^{G12V} expression increase the risk of liver tumor development. We therefore sought to address whether stable expression of *Nras*^{G12V} in CCR2 KO mouse livers results in increased liver tumor development (Figures 2C–2E). Indeed, when CCR2 KO and wild-type mice were followed up long term after stable delivery of oncogenic *Nras*, we found that CCR2 KO mice developed lethal multifocal HCC as early as 6 months after intrahepatic *Nras*^{G12V} expression. In comparison, wild-type mice showed no tumor development and survived. In summary, these data suggest that CCL2-CCR2 signaling acts as tumor suppressive in early stages of liver tumorigenesis by (1) enabling monocyte/macrophage-dependent immune surveillance of pre-cancerous senescent hepatocytes and (2) an immune cell-mediated enhancement of senescence induction, which is independent of CCR2 expression on hepatocytes. While our previous work suggests that liver carcinomas can arise from pre-cancerous hepatocytes after bypassing a senescence arrest (Kang et al., 2011), our present data from the CCR2-deficient model does not allow discrimination of whether liver carcinomas arise from previously senescent cells or from cells that have failed to undergo a full senescence response.

Peritumoral Cellular Senescence Promotes Growth of Liver Tumors in Mice

HCCs develop in chronically damaged livers, in which fully established tumor cells, and senescent hepatocytes and non-parenchymal cells, co-exist (Jurk et al., 2014; Krizhanovsky et al., 2008). Therefore, we studied hepatic senescence-associated CCL2-CCR2 signaling during later phases of liver tumor development, namely in a setting where fully transformed HCC cells give rise to hepatocellular carcinomas within a liver harboring senescent hepatocytes. To this end, cellular senescence was induced in wild-type mouse livers by hydrodynamic delivery of transposable elements encoding *Nras*^{G12V}. Hydrodynamic delivery of *Nras*^{D38A} served as a control. After hepatic senescence induction, we seeded luciferase-expressing syngeneic HCC cells into the liver via splenic injection (Figure 3A). Luciferase imaging of liver explants and weight measurement of tumors (including non-tumorous liver tissue) revealed that senescent mouse livers harbored a significantly higher tumor mass than the non-senescent livers (Figures 3B–3E). Furthermore, seeding a reduced number of HCC cells yielded more macroscopically visible tumors in *Nras*^{G12V}-injected compared with *Nras*^{D38A}-injected mice (Figures 3F and 3G), indicating that cellular senescence in non-tumor tissue accelerated growth of liver tumors. These results were confirmed using an independent liver cancer cell line (BNL), which was seeded into syngeneic BALB/c mice (Figures S4A–S4C). Histopathological quantification of tumor nodules revealed more BNL tumors in *Nras*^{G12V}-injected than in with *Nras*^{D38A}-injected mice. Therefore, cellular senescence in peritumoral liver tissue promotes growth of murine HCC.

Senescence-Associated Gene Signature in Peritumoral Tissue Is Associated with Poor Survival and Early Recurrence in HCC Patients

Next, we studied human tissue specimens from HCC patients to corroborate our findings in patient-derived samples, in which senescence is induced by chronic inflammation. Chronic inflammation is associated with repetitive waves of hepatocyte death and compensatory proliferation, which can trigger replicative senescence or, via an aberrant activation of oncogenes, oncogene-induced senescence. We analyzed samples derived from a cohort of 247 Chinese HCC patients (Roessler et al., 2010). We utilized previously described (Yildiz et al., 2013) liver tumor cell-related and senescence-associated gene signatures to determine whether their expression patterns in peritumoral liver tissues was associated with survival of HCC patients (Table S1). We found that senescence-associated gene expression (senescence high risk) in peritumoral tissue correlated with worse overall survival and shorter recurrence-free survival compared with patients without a senescence peritumoral tissue gene signature (senescence low risk) (Figure 4A). Consistent results were obtained in a second independent patient cohort (Figure S5). In addition, we found that the senescence gene signature was associated with both early and late recurrence (Figure 4B). Next, we performed a hierarchical cluster analysis, which separated all HCC cases into three groups, with clusters A and B enriching senescence high-risk cases (Figure 4C).

We then asked whether the tumor biology could account for the observed differences in survival and recurrence, and

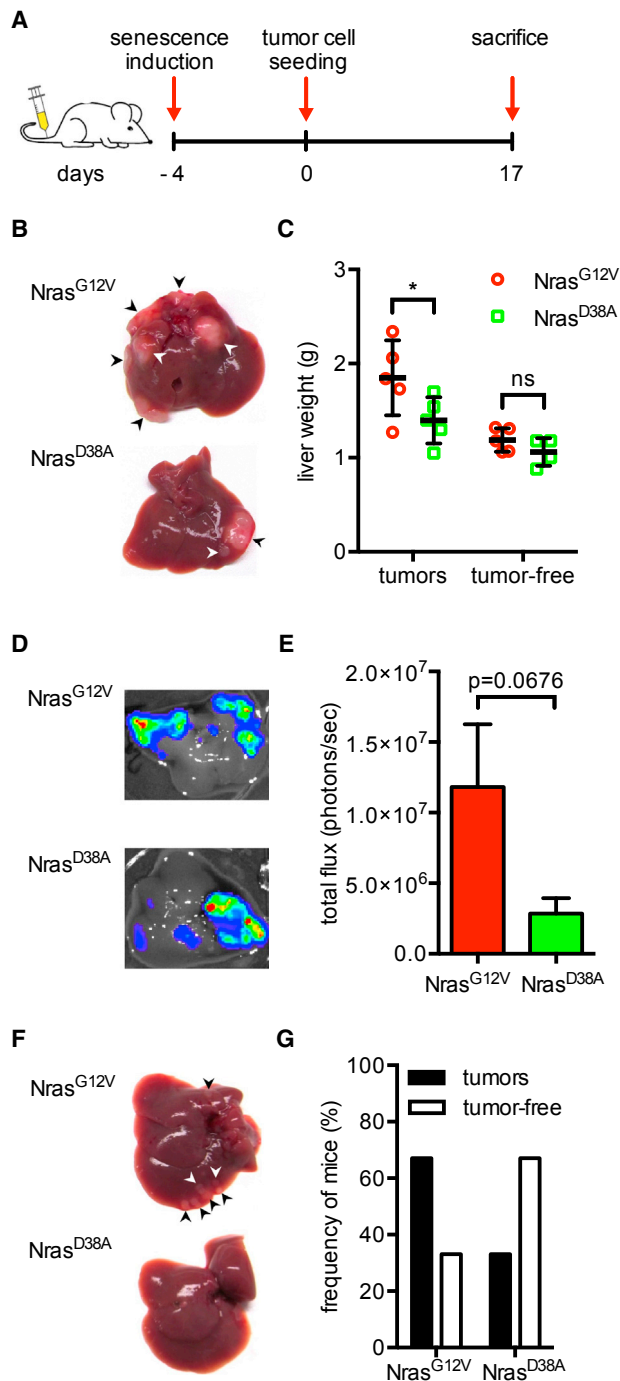


Figure 3. Peritumoral Senescence Promotes Tumor Growth of Murine Liver Carcinomas

(A) Schematic representation of the experimental protocol. Four days after hydrodynamic injection, either 1×10^5 or 3×10^5 RIL175 cells were seeded into the liver via intrasplenic injection and mice were euthanized 17 days after tumor cell seeding.

(B) Macroscopic images of mouse livers after 3×10^5 RIL175 cells were seeded into *Nras*^{G12V} or *Nras*^{D38A}-injected mice. Arrowheads indicate tumor nodules.

(C) Liver weight of *Nras*^{G12V}- or *Nras*^{D38A}-injected mice with or without tumor seeding depicted in (B); $n = 5$ mice per group.

(D) Representative bioluminescence images of livers 17 days after tumor cell seeding in *Nras*^{G12V}- or *Nras*^{D38A}-injected mice.

analyzed the gene expression profiles of tumors of senescence high-risk and senescence low-risk groups. A class-comparison analysis revealed that only 31 genes were differentially expressed in tumor tissue (univariate $p < 0.001$) and only one gene (*YARS*, tyrosyl-tRNA-synthetase) was significant when adjusted by multiple test (false discovery rate [FDR] < 0.05), suggesting that the observed differences in survival were unlikely to be explained by differences in tumor biology. We performed univariate and multivariate Cox proportional hazards regression analyses to determine whether senescence-associated prognosis was confounded by other prognostic factors such as age, gender, and underlying liver diseases. Univariate analysis revealed that the senescence-associated gene signature as well as gender, cirrhosis, α -fetoprotein (AFP), tumor size, nodularity, vascular invasion, and tumor staging were significant predictors of survival (Table S2). A multivariate Cox regression model controlled for gender, cirrhosis, AFP, and tumor staging revealed a strong trend of the senescence-associated gene signature in peritumoral tissue to be independently associated with patient survival ($p = 0.092$). These data demonstrate that cellular senescence in peritumoral tissue negatively affects survival and tumor recurrence in patients with HCC, and supports our findings in mice that peritumoral senescence accelerates liver cancer growth (Figure 3).

Senescent Peritumoral Tissue Induces Immature Myeloid Cell-Mediated Natural Killer Cell Inhibition via CCL2-CCR2 Signaling, Promoting HCC Growth in Mice

It has been reported that cytokines secreted by senescent cells can directly promote proliferation of susceptible cancer cells via paracrine signaling (Krtolica et al., 2001; Kuilman et al., 2008, 2010). In mice, senescent hepatocytes overexpressing oncogenic *Nras*^{G12V} not only secrete CCL2, but also other chemokines and cytokines (Figure S1A). Accordingly, these factors could be responsible for the observed tumor growth promotion via augmentation of tumor cell proliferation or invasiveness. Thus, we isolated and cultured hepatocytes from *Nras*^{G12V}- or *Nras*^{D38A}-injected mice and collected the cell-culture supernatants to study their effects on mouse HCC cells (Figures S6A and S6B). Neither proliferation nor invasiveness of tumor cells was enhanced by the senescent cell-secreted cytokines, suggesting that the SASP had no direct tumor growth-promoting effect. We also found that the presence of senescent hepatocytes did not result in an increased engraftment of murine HCC cells, which were seeded into mouse livers after hydrodynamic gene delivery (Figure S6C).

Since senescent cell-secreted cytokines and chemokines were not directly responsible for the observed tumor growth

(E) Relative luminescence of liver tumors depicted in (D); $n = 15$ mice per group.

(F) Representative images of livers from mice that received 1×10^5 RIL175 cells, $n = 6$ mice per group. Arrowheads indicate macroscopically detected tumor nodules.

(G) Frequency of livers that did (black bars) or did not (white bars) show macroscopically visible tumors in *Nras*^{G12V}- or *Nras*^{D38A}-injected mice depicted in (F).

Values are mean \pm SD in (C) and mean \pm SEM in (E); * $p \leq 0.05$; ns, not significant, Two-way ANOVA was used in (C) and Student's *t* test in (E) to calculate statistical significance. Each experiment was performed ≥ 3 times with a total of $n \geq 5$ mice per group. See also Figure S4.

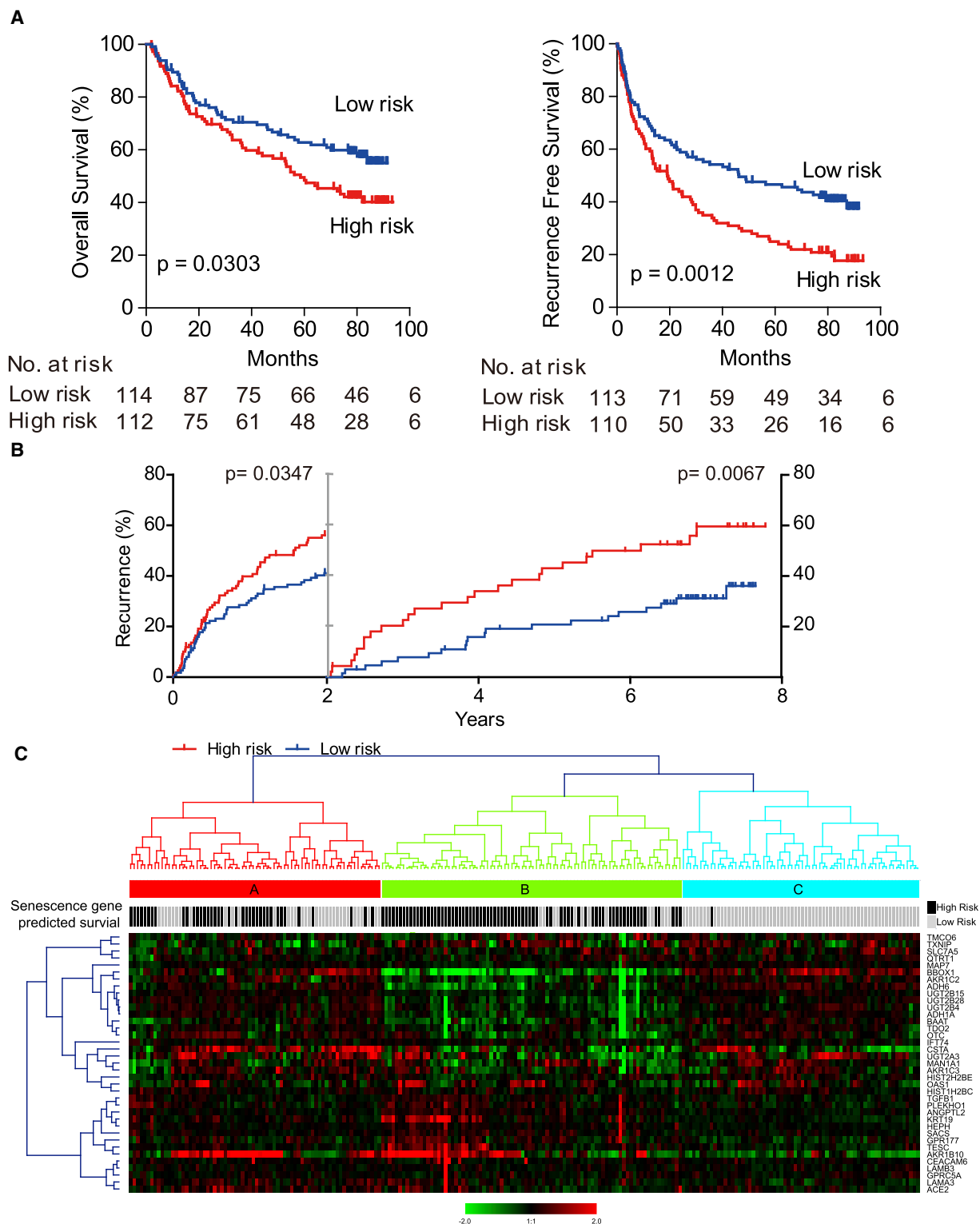


Figure 4. Senescence in Peritumoral Tissue Is Associated with Poor Survival in HCC Patients

(A) Kaplan-Meier survival analyses of 226 Chinese HCC cases based on survival risk prediction results of the senescence-associated gene signature in non-tumor tissue. Overall survival of 226 patients and recurrence-free survival of 223 HCC patients are shown.

(B) Tumor recurrence in 223 Chinese HCC cases described in (A).

(legend continued on next page)

promotion, we hypothesized that immunosuppressive myeloid cells could mediate the senescence-induced tumor growth promotion. In tumor-bearing mice, iMC and their subsets possess distinct immunosuppressive functions (Gabrilovich and Nagaraj, 2009). To assess whether senescence-recruited iMC in tumor-free mice also exhibit immunosuppressive capabilities, we isolated iMC from *Nras*^{G12V}-injected mouse livers and tested their ability to suppress CD8 T cell proliferation in vitro (Figures 5A and S6D). Indeed, CD8 T cell proliferation was inhibited by senescence-recruited hepatic iMC. Furthermore, suppression of T cell proliferation was mediated by an inducible nitric oxide synthase (iNOS)-dependent mechanism, as the immunosuppression was reversed after addition of an iNOS inhibitor (L-NMMA[N^G-monomethyl-L-arginine]), but not after addition of an arginase inhibitor (N-NOHA [N^ω-hydroxy-L-arginine]). In contrast, splenic iMC from mice with senescent livers did not accumulate nor were they immunosuppressive (Figure S6E), indicating that senescence-mediated effects on immune cells are restricted to senescent tissue.

Next, we depleted the iMC in senescent livers via anti-Gr-1 antibody administration before HCC cell seeding to confirm that immunosuppressive iMC mediated the senescence-induced tumor growth promotion. Weight of tumor-bearing *Nras*^{G12V}-injected livers in antibody-depleted mice was reduced to levels of *Nras*^{D38A}-injected mice (with or without depletion), indicating that absence of iMC abrogated the accelerated tumor growth observed in untreated *Nras*^{G12V}-injected wild-type mice (Figure 5B).

CCL2 is a well-known inducer of immunosuppressive iMC accumulation in tumor-bearing mice (Gabrilovich and Nagaraj, 2009) and it also induced the senescence-mediated expansion of iMC in our model (Figures 1 and S1). Hence, we hypothesized that senescence-mediated tumor growth promotion would be absent in CCR2 KO mice due to a lack of iMC accumulation. Again, tumor cells were seeded into senescent or non-senescent livers of CCR2 KO mice, and the quantification of tumor burden confirmed the abrogation of the senescence-induced tumor growth promotion (Figure 5B). Thus, immunosuppressive iMC accumulation via CCL2-CCR2 signaling during early liver tumor growth is responsible for senescence-induced tumor growth promotion in mice.

In HCC patients, iMC can suppress T cell and natural killer (NK) cell function (Hoechst et al., 2008, 2009). Accordingly, we sought to identify which lymphocyte population is inhibited by iMC in our model, and depleted different immune cell populations before seeding HCC cells into senescent livers. While the absence of CD4 T cells and NKT cells had no effect on tumor growth in *Nras*^{D38A}-injected mice, there was only a slight acceleration of tumor growth in CD8 T cell-depleted mice. In contrast, NK cell depletion caused accelerated tumor growth in *Nras*^{D38A}-injected non-senescent mice similar to senescence-induced tumor growth promotion (Figure 5C), suggesting that NK cells might be inhibited by senescence-recruited iMC in *Nras*^{G12V}-injected mice. To address this hypothesis, we set out to assess the

expression of markers that indicate activation or degranulation of NK cells in our tumor cell-seeding model. KLRG1 surface expression is upregulated upon NK cell activation (Sun and Lanier, 2011). CD107 is a marker for NK cell degranulation and cytotoxicity that lines the luminal surface of granules containing granzymes, and becomes temporarily expressed on the NK cell surface during exocytosis. During this brief surface expression, CD107 can be stained by antibodies in vivo, allowing the detection of degranulating cells (Yuzefpolskiy et al., 2015). Therefore, we measured activation and degranulation of NK cells in the presence or absence of iMC (Figures 5D–5H). We found that NK cells in senescent livers harboring tumor cells were activated, as demonstrated by the increase of KLRG1⁺CD107⁺ NK cells upon tumor cell seeding. However, when iMC were depleted by anti-Gr-1 antibody, significantly more NK cells were KLRG1⁺ and CD107⁺, confirming that iMC inhibited NK cell degranulation and activation (Figures 5E and 5F). Furthermore, the presence or absence of iMC did not alter absolute NK cell numbers in senescent livers containing tumor cells compared with livers of untreated wild-type control mice (Figure 5G). Together our data illustrate that senescence-recruited iMC inhibit NK cell anti-tumor function and thereby promote tumor growth.

Tumor Cells Inhibit Maturation of Monocytic iMC to Macrophages in Senescent Livers

Pre-cancerous senescent cells induce their own clearance through a recruitment of CCR2⁺ myeloid cells, which thereby prevent outgrowth of HCC (Figures 1 and 2). On the other hand, CCR2⁺ myeloid cells enhance the growth of liver tumors by inhibiting NK cells (Figure 5). Therefore, we sought to delineate the underlying mechanism of these two opposing functions of senescence-recruited myeloid cells.

Depletion of monocytic iMC or macrophages was shown to result in impaired senescent cell clearance (Kang et al., 2011). This suggests that either both cell types clear senescent cells or monocytic iMC are precursors of macrophages, which are the actual effector cells responsible for senescent cell clearance. In support of the latter concept, it has been shown that Ly6C^{hi} monocytes are recruited to the liver in a CCR2-dependent fashion and differentiate into Ly6C^{lo} macrophages (Zigmond et al., 2014). Thus, we quantified Ly6C^{hi} monocytes in the bone marrow in response to hydrodynamic delivery of *Nras*^{G12V} and found an expansion of these cells (Figure 6A), suggesting that the accumulating monocytic iMC in senescent livers are recruited from the bone marrow. Next, we adoptively transferred CD45.1⁺ Ly6C^{hi} monocytes, isolated from bone marrows of untreated wild-type mice, into *Nras*^{G12V}-injected CD45.2⁺ mice and analyzed the differentiation of transferred monocytes (Figures 6B–6F). Indeed, some of the transferred monocytes downregulated Ly6C and differentiated into macrophages, and the ratio of macrophages to monocytic iMC increased over time after transfer, demonstrating that monocytic iMC in fact give rise to macrophages in senescent livers. Therefore, in tumor-free livers

(C) Hierarchical clustering of 37 senescence-associated genes that are significantly associated with HCC survival. Each column represents an individual tissue sample. Genes were ordered by centered correlation and complete linkage. The scale represents gene expression levels from -2.0 to 2.0 in \log_2 scale. Each case status is categorized by the senescence-associated gene signature described in (A). See also Figure S5; Tables S1 and S2.

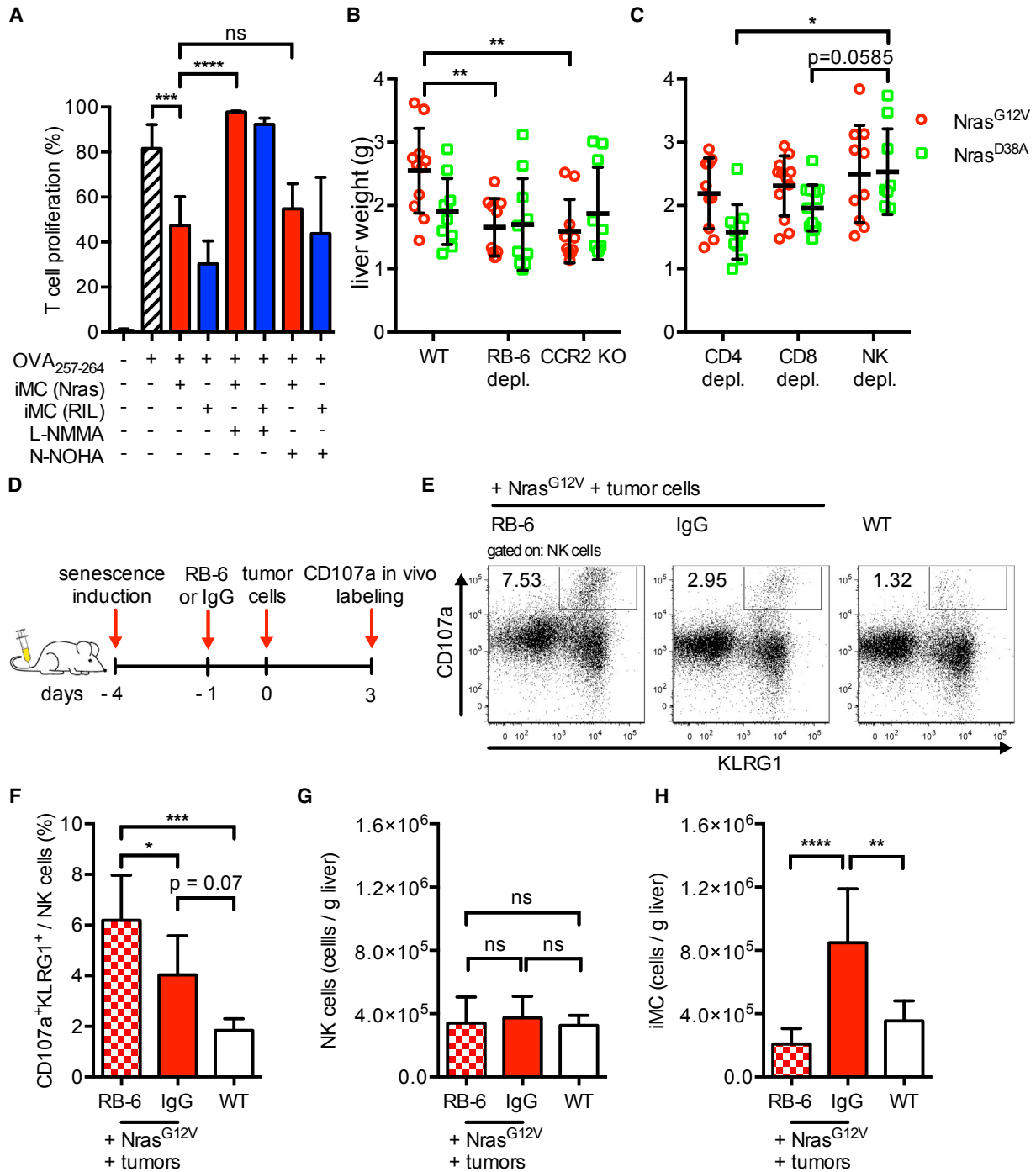


Figure 5. Senescence-Recruited CCR2⁺ Immunosuppressive Myeloid Cells Induce Liver Tumor Growth Promotion via NK Cell Inhibition
 (A) T cell proliferation inhibition by iMC assessed by flow cytometry. Hepatic CD11b⁺Gr-1⁺ cells were purified from *Nras*^{G12V}-injected (“Nras”) or subcutaneous RIL175 tumor-bearing mice (“RIL”), which served as positive controls, and co-incubated with 10⁵ OT-I cells at 1:1 ratio, in the presence of 0.1 μg/mL OVA₂₅₇₋₂₆₄ peptide. N-NOHA (0.5 mM) or L-NMMA (0.5 mM) were used to block activity of arginase and iNOS, respectively.

(B) Liver weight after gene delivery and tumor cell seeding with or without immature myeloid cell depletion in C57BL/6 wild-type (WT) mice or CCR2 KO mice. iMC were depleted 24 hr before RIL175 seeding by one-time administration of anti-Gr-1 antibody (clone: RB6-8C5), n ≥ 10 mice per group.

(C) Liver weight after hydrodynamic gene delivery and tumor cell seeding in C57BL/6 mice with depleted immune cells. CD4⁺ cells or CD8⁺ cells were depleted by intraperitoneal administration of 200 μg of GK1.5 antibody or 2.43 antibody 24 hr before and 7 days after RIL175 seeding, respectively. NK cells were depleted by intravenous injection of 600 μg of PK136 antibody 24 hr before and 1 and 4 days after RIL175 seeding, n ≥ 10 mice per group.

(D) Schematic representation of the experimental protocol for the NK cell degranulation assay with results depicted in (E) to (H). Three days after *Nras*^{G12V} injection, mice received either iMC-depleting anti-Gr-1 antibody (clone: RB6-8C5, “RB-6”) or immunoglobulin G antibody intraperitoneally, followed by seeding of (legend continued on next page)

senescent hepatocytes recruit monocytic iMC, which subsequently differentiate into macrophages.

In tumor-bearing hosts it has been shown that tumor cells secrete a variety of factors to inhibit myeloid cell differentiation into effector cells such as macrophages or dendritic cells (Gabrilovich et al., 2012; Strauss et al., 2015). Accordingly, when bone marrow Ly6C^{hi} monocytes were transferred into senescent livers containing tumor cells, the ratio of macrophages to monocytic iMC decreased in comparison with livers without tumor cells, suggesting that tumor cells inhibited maturation of monocytic iMC (Figures 6C–6F). Consequently, in senescent livers with tumor cells, the number of monocytic iMC increased while the number of macrophages decreased compared with senescent livers without tumor cells (Figure 6G).

When we compared the accumulation of the entire iMC population in *Nras*^{G12V}- or *Nras*^{D38A}-injected mice 7 days after senescence induction in mice with or without HCC cell seeding on day 4 (Figure 6H), we found significantly more iMC in senescent livers seeded with HCC cells compared with senescent livers without tumor cells. In contrast, only a small increase in iMC was observed in non-senescent livers 3 days after tumor cell seeding. Thus, tumor cells augmented the senescence-induced accumulation of iMC (Figure 6H), likely through the combined action of senescent cell- and tumor cell-secreted cytokines. On the other hand, senescent hepatocytes caused early accumulation of immunosuppressive myeloid cells. These iMC then inhibited NK cell activity to promote tumor growth (Figure 5). Furthermore, it is noteworthy that iMC-mediated NK cell inhibition does not interfere with senescent cell surveillance in tumor-free mice, because NK cells are not involved in clearance of pre-cancerous senescent hepatocytes (Kang et al., 2011).

Senescence in Peritumoral Tissue of HCC Patients Is Associated with Increased CCL2 Expression, Myeloid Cell Accumulation, and Reduced NK Cell Gene Activity

Our mouse data revealed that senescent hepatocytes secreted chemokines to amplify the tumor-induced iMC accumulation. Therefore, we asked whether the senescence gene expression signature in peritumoral tissue was also associated with an increase in chemokine gene expression in humans. Thus, we compared non-tumor senescence high- and low-risk groups by class-comparison analysis and found an increase of many chemokines (Figure 7A), including CCL2, CCL5, and CXCL1 ($p < 0.01$, FDR < 0.01), indicating that the senescence activity was associated with cytokine/chemokine expression. Hierarchical clustering of the 14 differentially expressed chemokine genes revealed a correlation of enhanced chemokine expression and senescence gene signature predicted survival (Figure 7B). It is important to note, however, that these factors could have been expressed not only by senescent hepatocytes but also by liver-infiltrating immune cells. Importantly, senescence-induced chemokines found in mouse hepatocytes (Figure S1A) were

also upregulated in the senescence high-risk group of peritumoral tissue of HCC patients (Figure 7B). Therefore, senescent peritumoral tissues of HCC patients as well as mouse senescent hepatocytes exhibit a similar SASP.

In mice, we found that SASP-mediated CCL2-CCR2 signaling triggered iMC accumulation, causing senescence-induced tumor growth promotion. Thus, we examined CCL2 expression and myeloid cell gene enrichment in peritumoral tissue in our cohorts of HCC patients. Among the three clusters from our hierarchical analysis (Figure 4C), CCL2 expression was significantly increased in the cluster that enriched for senescence gene predicted survival high-risk cases (Figure 7C), suggesting that CCL2 was also involved in the senescence-induced tumor growth promotion in humans.

Furthermore, immune cell-specific gene enrichment analysis in peritumoral tissue of human HCC showed significantly more myeloid-specific genes to be upregulated in the senescence high-risk group than in the low-risk group (Figure 7D). As liver tumors induce the accumulation of immunosuppressive myeloid cells irrespective of senescence (Hoechst et al., 2008), these data suggest that peritumoral senescence amplified the tumor-induced myeloid accumulation, likely through CCL2. To confirm the senescence-induced peritumoral CCR2⁺ myeloid cell accumulation, we performed immunohistochemistry for CCR2 expression, the myeloid cell marker CD68, and senescence-associated markers p16 and p21 in peritumoral liver tissue (Figures 7E and S7A). Expression of senescence markers correlated with an increase in myeloid cells. Moreover, myeloid cell expansion correlated with more abundant peritumoral CCR2 expression, indicating that peritumoral senescence indeed induced the accumulation of CCR2⁺ myeloid cells (Figures 7E and S7A).

Supporting the myeloid cell-mediated NK cell dysfunction we demonstrated in mice, we also found significant depletion in NK cell-specific gene activity (Figure 7D) in the immune cell-specific gene enrichment analysis in humans. Remarkably, class-comparison analysis showed a significant upregulation of PTGS2 (prostaglandin-endoperoxide synthase 2) and TGFB1 (transforming growth factor β 1) in the senescence high-risk group ($p < 0.01$, FDR < 0.01). This is noteworthy, because the former has consistently been implicated in the induction of immunosuppressive myeloid cells in cancer patients (Mao et al., 2013, 2014; Obermajer et al., 2011) and the latter has been shown to trigger myeloid cell-mediated NK cell inhibition (Li et al., 2009; Mao et al., 2014).

DISCUSSION

While cellular senescence is widely accepted as a potent cell-autonomous anti-cancer mechanism, it has been shown that senescent cell-secreted cytokines can exert context-dependent pro- as well as anti-tumor effects. Here, we show that the SASP of senescent hepatocytes promotes growth of HCC by

3×10^5 RIL175 tumor cells into the liver 24 hr later. Three days after tumor cell seeding, anti-CD107a-PE antibody was injected intravenously and 4 hr later, mice were euthanized and liver leukocytes isolated for analysis by flow cytometry ($n = 9$ mice per group). Untreated wild-type mice served as controls ($n = 4$ mice). (E–H) Representative dot plot of CD107a and KLRG1 staining on NK cells (E) and quantification of CD107a⁺KLRG1⁺ NK cells among all hepatic NK cells (F). Absolute number of cells per gram of liver tissue of NK cells (G) and iMC (H) quantified by flow cytometry.

Values are mean \pm SD; * $p \leq 0.05$, ** $p \leq 0.01$, *** $p \leq 0.001$, **** $p \leq 0.0001$; ns, not significant. One-way ANOVA was used in (A), (F), (G), and (H), and two-way ANOVA in (B) and (C) to calculate statistical significance. Each experiment was performed two or three times. See also Figure S6.

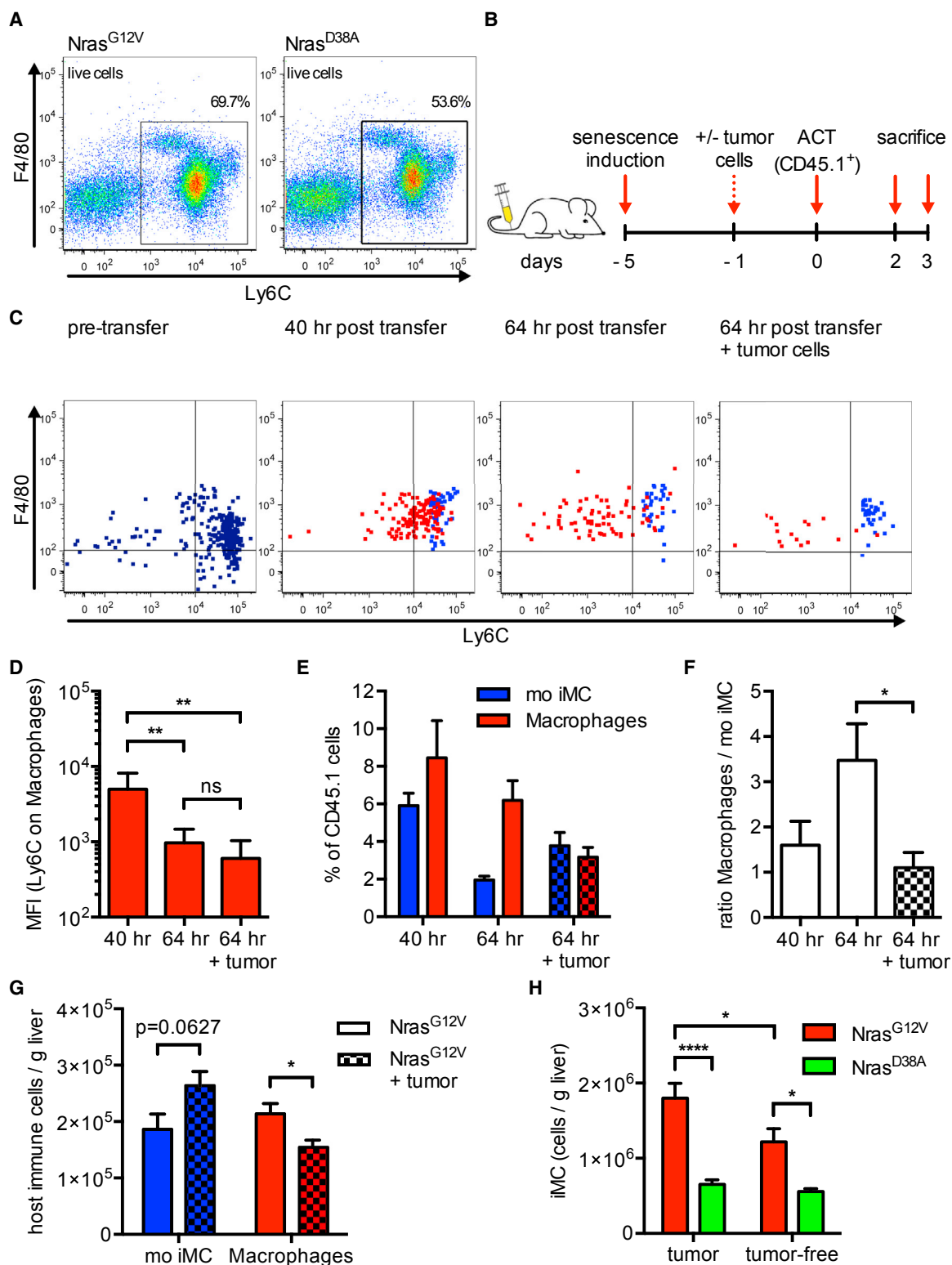


Figure 6. Tumor Cells Inhibit Maturation of Monocytic iMC to Macrophages in Senescent Livers

(A) Quantification of Ly6C⁺ monocytes by flow cytometry from bone marrows after hydrodynamic delivery of indicated genes in C57BL/6 mice. Gated on live cells. (B) Schematic representation of the experimental protocol for results depicted in (C) to (G). Five days after hydrodynamic *Nras*^{G12V} delivery, CD45.1⁺ bone marrow monocytes from untreated wild-type mice were intravenously injected into mice with or without 3×10^5 RIL175 tumor cell seeding 24 hr prior. Mice were

(legend continued on next page)

inhibiting NK cell function through immunosuppressive immature myeloid cell accumulation, thereby fueling growth of murine and human HCC and worsening the survival of human HCC patients. In both mice and humans, peritumoral tissue senescence accelerated tumor growth or decreased overall and recurrence-free survival, respectively. Moreover, in either species, myeloid cell-mediated NK cell inhibition was identified to be responsible for the observed effects. In contrast, senescence-induced myeloid cell accumulation is also necessary for the removal of pre-cancerous senescent cell protection from tumor initiation. Thus, our data demonstrate a dual context-dependent function of CCL2-CCR2 signaling in HCC initiation and progression (Figure S7B). Our findings harbor direct translational impact for the treatment of patients with liver diseases, because CCR2 antagonists are being clinically evaluated as a possible treatment option for various disease conditions, including inflammatory, metabolic, and vascular diseases (Struthers and Pasternak, 2010). As particular patients with metabolic syndrome and cardiovascular disease often suffer from non-alcoholic fatty liver disease or non-alcoholic steatohepatitis, our data caution against administration of CCR2 antagonists in such patients, as HCC development may be fueled. In contrast, once HCCs have developed, the CCL2-CCR2 axis constitutes an actionable target to inhibit myeloid cell-mediated immunosuppression of anti-tumor immune responses.

The factor responsible for the amplification of immunosuppressive iMC accumulation as well as myeloid cell-mediated senescent cell clearance was identified to be CCL2, which has been reported to be part of the SASP (Acosta et al., 2013; Kang et al., 2011; Toso et al., 2014) and functions as a chemokine to attract immune cells expressing the receptor CCR2 (Deshmane et al., 2009). This chemokine has been implicated in tumor growth promotion as well as inhibitory effects (Conti and Rollins, 2004; Li et al., 2013; Qian et al., 2011; Schneider et al., 2012). Our study reveals distinct functions of the CCL2-CCR2 axis in early stages of liver tumor development versus later stages of liver tumor progression. This seemingly contradictory phenomenon can be explained by the plasticity of CCR2⁺ myeloid cells, which carry out effector functions of the CCL2-CCR2 axis. Myeloid cells, more specifically monocytes, can possess immunosuppressive properties, but can also differentiate into pro-inflammatory macrophages upon entry into their end-organ tissue, depending on the cytokine milieu and the microenvironment they encounter (Gabrilovich and Nagaraj, 2009; Gabrilovich et al., 2012). Indeed, we have shown that immune surveillance

of senescent pre-cancerous hepatocytes is dependent on tissue resident macrophages, which are replenished by infiltrating monocytes. However, if tumor cells impede the maturation of infiltrating monocytes into macrophages through tumor-secreted cytokines, the monocytes retain their immunosuppressive function and contribute to tumor immune escape.

It is important to point out that our murine data are based on a model of oncogene-induced senescence, whereas senescence in peritumoral human tissue is triggered by chronic inflammation, causing both replicative and oncogene-induced senescence. Furthermore, tumor development in mice was triggered by tumor cell seeding throughout the entire liver, while human carcinomas developed spontaneously in the chronically damaged liver. Despite these differences between the human data and the employed mouse model, both human and murine senescent liver tissue exhibited a similar senescence-induced chemokine-secretion profile, resulting in myeloid cell accumulation and promotion of tumor growth.

The ability of the SASP to induce an immunosuppressive immune cell environment has recently been shown in a mouse model of Pten-loss-induced cellular senescence in prostates with prostatic intraepithelial neoplasia (Toso et al., 2014). In this study, the immunosuppressive myeloid cells impeded senescence surveillance and consequently facilitated senescent tumor cell survival, which after senescence escape and cell-cycle re-entry ultimately led to progression to invasive adenocarcinomas. Whereas the aforementioned report elucidated the involvement of immunosuppressive myeloid cells in aiding malignant cell transformation, our data reveal that oncogene-induced cellular senescence amplifies the accumulation of immunosuppressive myeloid cells in peritumoral tissue of an existing tumor. These accumulating suppressive myeloid cells inhibit NK cells and thereby promote tumor growth. In patients with HCC, there is a wealth of information on myeloid cell-mediated NK cell dysfunction as well as the importance of NK cells in controlling HCC growth (Cai et al., 2008; Hoechst et al., 2009; Taketomi et al., 1998; Wu et al., 2013). For example, it has been shown that immunosuppressive myeloid cells accumulate in patients with HCC and inhibit NK cell cytokine production, and target cell killing via the NKp30 receptor (Hoechst et al., 2009). Here, we extend these studies by demonstrating that in patients with peritumoral senescence immunosuppressive myeloid cell accumulation is enhanced, leading to inhibition of NK cell activity.

Our findings highlight the opposing functions of the SASP as a pro- as well as anti-cancer mechanism. Therefore, so-called

ethanized 40 hr (2 days) or 64 hr (3 days) after adoptive monocyte transfer, and hepatic myeloid cells were analyzed by flow cytometry. ACT, adoptive cell transfer.

(C) Representative dot-plot analysis of hepatic CD45.1⁺ cells in experimental setup depicted in (B). Dot-plot color code illustrates cell gate: purple dots, CD45.1⁺ live cells (post bone marrow monocyte isolation); blue dots, CD45.1⁺ mo iMC; red dots, CD45.1⁺ macrophages.

(D) Mean fluorescent intensity (MFI) of Ly6C expression on macrophages.

(E) Quantification of CD45.1⁺ mo iMC and CD45.1⁺ macrophages via flow cytometry.

(F) Ratio of CD45.1⁺ Macrophages/CD45.1⁺ mo iMC calculated from results depicted in (E).

(G) The total cell number per gram of liver tissue of host (CD45.2⁺) mo iMC and macrophages 64 hr after adoptive cell transfer into mice receiving indicated treatment.

(H) Quantification of immature myeloid cell accumulation by flow cytometry 7 days after delivery of indicated genes with or without RIL175 seeding on day 4. These mice did not receive adoptively transferred monocytes.

Values are mean \pm SEM; * $p \leq 0.05$, ** $p \leq 0.01$, **** $p \leq 0.0001$; ns, not significant. One-way ANOVA was used in (D) and (F), two-way ANOVA in (H), and Student's *t* test in (G) to calculate statistical significance. Each experiment was performed two or three times with $n = 4$ (40-hr group), $n \geq 6$ (64-hr groups), and $n \geq 9$ (H) mice per group.

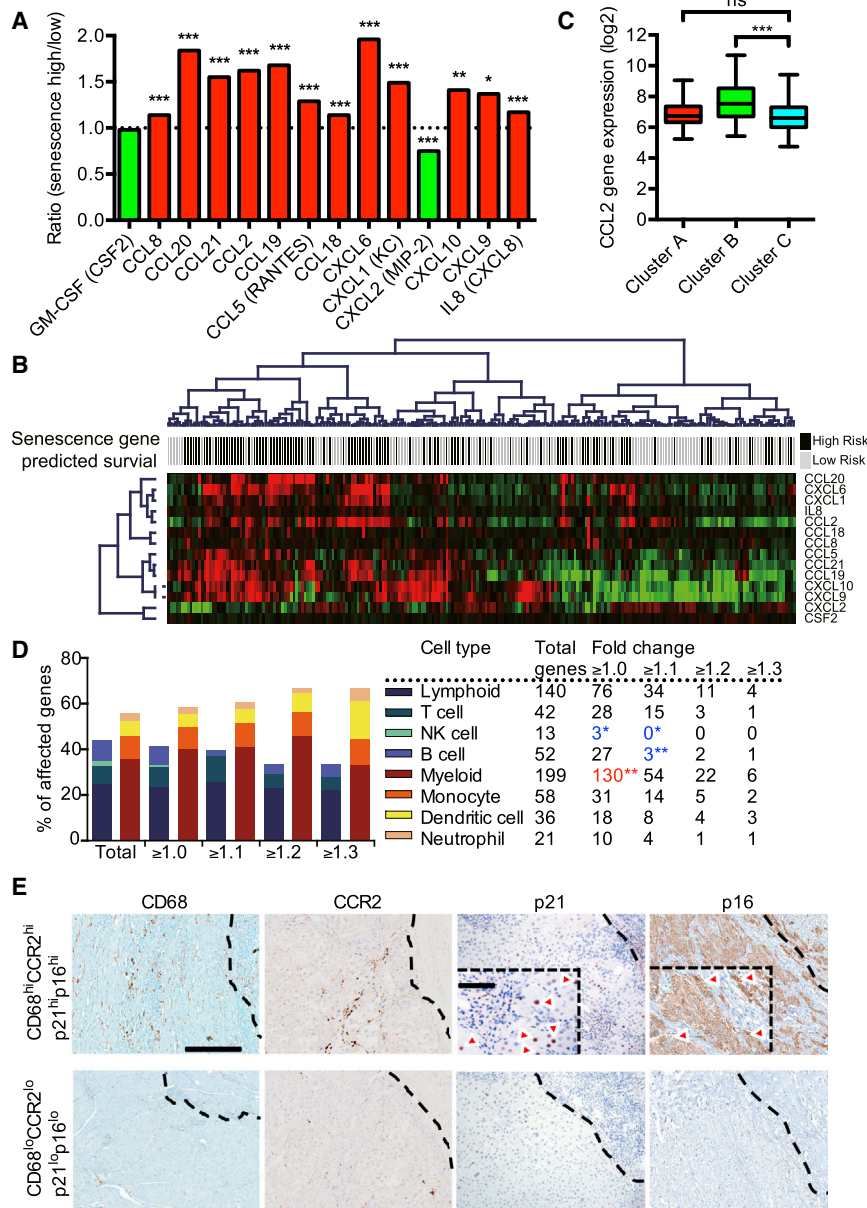


Figure 7. Increased Chemokine Expression and Myeloid Cell Accumulation in Senescent Peritumoral Tissue of HCC Patients

(A) Results of a class-comparison analysis between senescence high- and low-risk groups reported in Figure 4A revealed significant differential expression of 14 chemokine genes ($p < 0.01$, FDR < 0.01).

(B) Hierarchical clustering of 14 chemokine genes reported in (A) and senescence gene signature predicted survival. Each column represents an individual tissue sample. Genes were ordered by centered correlation and complete linkage. The scale represents gene expression levels from -2.0 to 2.0 in \log_2 scale. Each case status is categorized by the senescence-associated gene signature described in Figure 4A.

(C) Expression of the CCL2 gene in three patient groups identified by hierarchical clustering shown in Figure 4B.

(D) Immune cell gene expression profiles based on senescence high- and low-risk subgroups defined by the senescence-associated gene signature. Among 1,622 immune cell genes defined by IRIS, 535 genes unique for each cell type were used to calculate the percentage of affected genes. The total number of significantly expressed genes (adjusted $p < 0.05$) with different fold changes is indicated. Blue numbers indicate significant gene depletion. Red number indicates significant gene enrichment.

(E) Immunohistochemistry staining for myeloid cells (CD68), CCR2⁺ cells, and senescent cells (p21 and p16) in peritumoral tissue of patients with HCC. Red arrows indicate p21- or p16-positive cells, respectively (scale bar, 100 μm ; scale bar within rectangular inlay in p21 and p16 stainings, 25 μm). Representative images are shown for one patient each with either high or low abundance of peritumoral myeloid and senescent cells. Dotted lines represent the tumor margin, with tumor tissue shown in the upper right corner of each image.

Values are mean \pm SD; * $p \leq 0.05$, ** $p \leq 0.01$, *** $p \leq 0.001$; ns, not significant. See also Figure S7.

pro-senescence therapy (Acosta and Gil, 2012; Nardella et al., 2011) for cancer treatment needs to ensure that the ensuing SASP promotes anti-tumor immunity. This could be achieved by reprogramming the SASP from pro- toward anti-cancer effector function (Toso et al., 2014). Moreover, pharmacological disruption of these SASP-mediated effector functions, e.g., through CCR2 antagonists, needs to be carefully discussed in patients with chronic liver disease in comparison with established HCC.

EXPERIMENTAL PROCEDURES

Mice, Cell Line, and Transposon System

Eight-week-old female CD45.2⁺ C57BL/6 mice or CD45.2⁺ *Ccr2*^{-/-} mice ("CCR2 KO") were used in all experiments, except for the BNL cell-seeding

experiment (Figures S4A–S4C), in which BALB/c mice were used. The transposon system encoding for oncogenic *Nras*^{G12V} (abbreviated as "Nras") or an effector loop mutant, *Nras*^{G12V/D38A} (abbreviated as "Nras^{D38A}"), were previously described (Kang et al., 2011). All experiments were conducted according to local institutional guidelines and were approved by either the Animal Care and Use Committee of the NIH or the authorities of the states of Lower Saxony (Niedersaechsisches Landesamt für Verbraucherschutz und Lebensmittelsicherheit) and Baden-Wuerttemberg (Regierungspraesidium Tübingen).

Animal Studies

For intrahepatic delivery of the transposon system (Kang et al., 2011), mice were hydrodynamically injected with a 5:1 molar ratio of transposon to transposase-encoding plasmid (30 μg total DNA) via the tail vein. Intrahepatic seeding of tumor cells was achieved by intrasplenic injection of 3×10^5 (or 1×10^5) RIL175 cells or 3×10^5 BNL cells, 4 days after hydrodynamic gene delivery. Livers were collected for analysis by histology or immunohistochemistry.

Alternatively, livers were processed for isolation of liver-infiltrating immune cells and subsequent analysis by flow cytometry. We refer to senescent non-tumor cells throughout the whole mouse liver in our mouse tumor cell-seeding studies as “peritumoral senescence.”

Statistical Analysis for Mouse Studies

Data were analyzed for statistical significance using Prism software (GraphPad). Kaplan-Meier plots and log-rank test were used to determine significance between survival curves. Significance for other data was tested using Student's *t* test, one-way ANOVA, or two-way ANOVA as indicated. *p* < 0.05 was considered to be statistically significant.

Human Hepatocellular Senescence Gene List

Deregulated genes in immortal Huh7 clones versus senescent Huh7 clones (Yildiz et al., 2013) were used as the hepatocellular senescence gene signature in the present study (Table S1).

Clinical Specimens, Microarray, and Statistical Analyses of Human Data

A previously described cohort of 247 Chinese HCC patients obtained with informed consent from patients at the Liver Cancer Institute (LCI) and Zhongshan Hospital (Fudan University) with publicly available Affymetrix U133A array data (NCBI GEO accession number GEO: GSE14520) was used to evaluate the prognostic correlation of the hepatocellular senescence gene signature for HCC patients (Roessler et al., 2010). We refer to the non-cancerous liver tissue directly adjacent to the tumor in these human datasets as “peritumoral tissue.”

More detailed information about the above procedures can be found in the Supplemental Experimental Procedures.

SUPPLEMENTAL INFORMATION

Supplemental Information includes Supplemental Experimental Procedures, seven figures, and two tables and can be found with this article online at <http://dx.doi.org/10.1016/j.ccell.2016.09.003>.

AUTHOR CONTRIBUTIONS

T.E., T.Y., and K.W. performed experiments. T.E., T.F.G., T.Y., and L.Z. designed the experiments and analyzed data. C.M., J.M.-E., S.K., F.R., T.L., and M.H. assisted with experiments and analysis or provided valuable reagents. J.J., M.F., and X.W.W. provided and T.E., J.J., and X.W.W. analyzed human data. T.E., T.F.G., and L.Z. conceived and designed the project. T.E., T.F.G., and L.Z. wrote the manuscript with all authors contributing to writing and providing feedback. L.Z. and T.F.G. contributed equally.

ACKNOWLEDGMENTS

This work was supported by the German Research Foundation (DFG; grants FOR2314 [L.Z.] and SFB685 [L.Z.]), the Gottfried Wilhelm Leibniz Program (L.Z.), the European Research Council (projects ‘CholangioConcept’ [L.Z.], ‘Heptromic’ [L.Z.]), the German Ministry for Education and Research (BMBF) (eMed [Multiscale HCC]) (L.Z.), the German Universities Excellence Initiative (third funding line: ‘future concept’) (L.Z.), the German Center for Translational Cancer Research (DKTK) (L.Z.), and the German-Israeli Cooperation in Cancer Research (DKFZ-MOST) (L.Z.). M.H. was supported by an ERC starting grant (LiverCancer mechanism), the Stiftung Experimentelle Biomedizin (Hofschneider Stiftung), the Pre-clinical Comprehensive Center (PCCC), and the Helmholtz foundation. T.F.G. and X.W.W. were supported by the Intramural Research Program of the NIH, NCI. We thank Dr. Michael J. Kruhlak (NIH) for technical assistance with scanning of liver section slides and Florian Heinzmann (University Hospital, Tübingen) for the generation of knockdown validated shRNAs.

Received: June 15, 2015

Revised: March 28, 2016

Accepted: September 12, 2016

Published: October 10, 2016

REFERENCES

- Acosta, J.C., and Gil, J. (2012). Senescence: a new weapon for cancer therapy. *Trends Cell Biol.* 22, 211–219.
- Acosta, J.C., O’Loughlen, A., Banito, A., Guijarro, M.V., Augert, A., Raguz, S., Fumagalli, M., Da Costa, M., Brown, C., Popov, N., et al. (2008). Chemokine signaling via the CXCR2 receptor reinforces senescence. *Cell* 133, 1006–1018.
- Acosta, J.C., Banito, A., Wuestefeld, T., Georgilias, A., Janich, P., Morton, J.P., Athineos, D., Kang, T.W., Lasitschka, F., Andriulis, M., et al. (2013). A complex secretory program orchestrated by the inflammasome controls paracrine senescence. *Nat. Cell Biol.* 15, 978–990.
- Cai, L., Zhang, Z., Zhou, L., Wang, H., Fu, J., Zhang, S., Shi, M., Zhang, H., Yang, Y., Wu, H., et al. (2008). Functional impairment in circulating and intra-hepatic NK cells and relative mechanism in hepatocellular carcinoma patients. *Clin. Immunol.* 129, 428–437.
- Conti, I., and Rollins, B.J. (2004). CCL2 (monocyte chemoattractant protein-1) and cancer. *Semin. Cancer Biol.* 14, 149–154.
- Coppe, J.P., Desprez, P.Y., Krtolica, A., and Campisi, J. (2010). The senescence-associated secretory phenotype: the dark side of tumor suppression. *Annu. Rev. Pathol.* 5, 99–118.
- Deshmane, S.L., Kremlev, S., Amini, S., and Sawaya, B.E. (2009). Monocyte chemoattractant protein-1 (MCP-1): an overview. *J. Interferon Cytokine Res.* 29, 313–326.
- Gabrilovich, D.I., and Nagaraj, S. (2009). Myeloid-derived suppressor cells as regulators of the immune system. *Nat. Rev. Immunol.* 9, 162–174.
- Gabrilovich, D.I., Ostrand-Rosenberg, S., and Bronte, V. (2012). Coordinated regulation of myeloid cells by tumours. *Nat. Rev. Immunol.* 12, 253–268.
- Hoechst, B., Ormandy, L.A., Ballmaier, M., Lehner, F., Kruger, C., Manns, M.P., Greten, T.F., and Korangy, F. (2008). A new population of myeloid-derived suppressor cells in hepatocellular carcinoma induces CD4(+)CD25(+)Foxp3(+) T cells. *Gastroenterology* 135, 234–243.
- Hoechst, B., Voigtlaender, T., Ormandy, L., Gamrekelashvili, J., Zhao, F., Wedemeyer, H., Lehner, F., Manns, M.P., Greten, T.F., and Korangy, F. (2009). Myeloid derived suppressor cells inhibit natural killer cells in patients with hepatocellular carcinoma via the NKp30 receptor. *Hepatology* 50, 799–807.
- Iannello, A., Thompson, T.W., Ardolino, M., Lowe, S.W., and Rautel, D.H. (2013). p53-dependent chemokine production by senescent tumor cells supports NKG2D-dependent tumor elimination by natural killer cells. *J. Exp. Med.* 210, 2057–2069.
- Jackson, J.G., Pant, V., Li, Q., Chang, L.L., Quintas-Cardama, A., Garza, D., Tavana, O., Yang, P., Manshour, T., Li, Y., et al. (2012). p53-mediated senescence impairs the apoptotic response to chemotherapy and clinical outcome in breast cancer. *Cancer Cell* 21, 793–806.
- Jurk, D., Wilson, C., Passos, J.F., Oakley, F., Correia-Melo, C., Greaves, L., Saretzki, G., Fox, C., Lawless, C., Anderson, R., et al. (2014). Chronic inflammation induces telomere dysfunction and accelerates ageing in mice. *Nat. Commun.* 2, 4172.
- Kang, T.W., Yevsa, T., Woller, N., Hoenicke, L., Wuestefeld, T., Dauch, D., Hohmeyer, A., Gereke, M., Rudalska, R., Potapova, A., et al. (2011). Senescence surveillance of pre-malignant hepatocytes limits liver cancer development. *Nature* 479, 547–551.
- Krizhanovskiy, V., Yon, M., Dickins, R.A., Hearn, S., Simon, J., Miething, C., Yee, H., Zender, L., and Lowe, S.W. (2008). Senescence of activated stellate cells limits liver fibrosis. *Cell* 134, 657–667.
- Krtolica, A., Parrinello, S., Lockett, S., Desprez, P.Y., and Campisi, J. (2001). Senescent fibroblasts promote epithelial cell growth and tumorigenesis: a link between cancer and aging. *Proc. Natl. Acad. Sci. USA* 98, 12072–12077.
- Kuilman, T., Michaloglou, C., Vredeveld, L.C., Douma, S., van Doorn, R., Desmet, C.J., Aarden, L.A., Mooi, W.J., and Peeper, D.S. (2008). Oncogene-induced senescence relayed by an interleukin-dependent inflammatory network. *Cell* 133, 1019–1031.
- Kuilman, T., Michaloglou, C., Mooi, W.J., and Peeper, D.S. (2010). The essence of senescence. *Genes Dev.* 24, 2463–2479.

- Li, H., Han, Y., Guo, Q., Zhang, M., and Cao, X. (2009). Cancer-expanded myeloid-derived suppressor cells induce anergy of NK cells through membrane-bound TGF- β 1. *J. Immunol.* *182*, 240–249.
- Li, M., Knight, D.A., A Snyder, L., Smyth, M.J., and Stewart, T.J. (2013). A role for CCL2 in both tumor progression and immunosurveillance. *Oncoimmunology* *2*, e25474.
- Lujambio, A., Akkari, L., Simon, J., Grace, D., Tschaharganeh, D.F., Bolden, J.E., Zhao, Z., Thapar, V., Joyce, J.A., Krizhanovsky, V., and Lowe, S.W. (2013). Non-cell-autonomous tumor suppression by p53. *Cell* *153*, 449–460.
- Mao, Y., Poschke, I., Wennerberg, E., Pico de Coana, Y., Egyhazi Brage, S., Schultz, I., Hansson, J., Masucci, G., Lundqvist, A., and Kiessling, R. (2013). Melanoma-educated CD14+ cells acquire a myeloid-derived suppressor cell phenotype through COX-2-dependent mechanisms. *Cancer Res.* *73*, 3877–3887.
- Mao, Y., Sarhan, D., Steven, A., Seliger, B., Kiessling, R., and Lundqvist, A. (2014). Inhibition of tumor-derived prostaglandin-e2 blocks the induction of myeloid-derived suppressor cells and recovers natural killer cell activity. *Clin. Cancer Res.* *20*, 4096–4106.
- Mudbhary, R., Hoshida, Y., Chernyavskaya, Y., Jacob, V., Villanueva, A., Fiel, M.I., Chen, X., Kojima, K., Thung, S., Bronson, R.T., et al. (2014). UHRF1 overexpression drives DNA hypomethylation and hepatocellular carcinoma. *Cancer Cell* *25*, 196–209.
- Nardella, C., Clohessy, J.G., Alimonti, A., and Pandolfi, P.P. (2011). Pro-senescence therapy for cancer treatment. *Nat. Rev. Cancer* *11*, 503–511.
- Obermajer, N., Muthuswamy, R., Lesnock, J., Edwards, R.P., and Kalinski, P. (2011). Positive feedback between PGE2 and COX2 redirects the differentiation of human dendritic cells toward stable myeloid-derived suppressor cells. *Blood* *118*, 5498–5505.
- Qian, B.Z., Li, J., Zhang, H., Kitamura, T., Zhang, J., Campion, L.R., Kaiser, E.A., Snyder, L.A., and Pollard, J.W. (2011). CCL2 recruits inflammatory monocytes to facilitate breast-tumour metastasis. *Nature* *475*, 222–225.
- Roessler, S., Jia, H.L., Budhu, A., Forgues, M., Ye, Q.H., Lee, J.S., Thorgeirsson, S.S., Sun, Z., Tang, Z.Y., Qin, L.X., and Wang, X.W. (2010). A unique metastasis gene signature enables prediction of tumor relapse in early-stage hepatocellular carcinoma patients. *Cancer Res.* *70*, 10202–10212.
- Schneider, C., Teufel, A., Yevsa, T., Staib, F., Hohmeyer, A., Walenda, G., Zimmermann, H.W., Vucur, M., Huss, S., Gassler, N., et al. (2012). Adaptive immunity suppresses formation and progression of diethylnitrosamine-induced liver cancer. *Gut* *61*, 1733–1743.
- Strauss, L., Sangaletti, S., Consonni, F.M., Szebeni, G., Morlacchi, S., Totaro, M.G., Porta, C., Anselmo, A., Tartari, S., Doni, A., et al. (2015). RORC1 regulates tumor-promoting “emergency” granulo-monocytopoiesis. *Cancer Cell* *28*, 253–269.
- Struthers, M., and Pasternak, A. (2010). CCR2 antagonists. *Curr. Top. Med. Chem.* *10*, 1278–1298.
- Sun, J.C., and Lanier, L.L. (2011). NK cell development, homeostasis and function: parallels with CD8(+) T cells. *Nat. Rev. Immunol.* *11*, 645–657.
- Takekomi, A., Shimada, M., Shirabe, K., Kajiyama, K., Gion, T., and Sugimachi, K. (1998). Natural killer cell activity in patients with hepatocellular carcinoma: a new prognostic indicator after hepatectomy. *Cancer* *83*, 58–63.
- Toso, A., Revandkar, A., Di Mitri, D., Guccini, I., Proietti, M., Sarti, M., Pinton, S., Zhang, J., Kalathur, M., Civenni, G., et al. (2014). Enhancing chemotherapy efficacy in Pten-deficient prostate tumors by activating the senescence-associated antitumor immunity. *Cell Rep.* *9*, 75–89.
- Wu, Y., Kuang, D.M., Pan, W.D., Wan, Y.L., Lao, X.M., Wang, D., Li, X.F., and Zheng, L. (2013). Monocyte/macrophage-elicited natural killer cell dysfunction in hepatocellular carcinoma is mediated by CD48/2B4 interactions. *Hepatology* *57*, 1107–1116.
- Xue, W., Zender, L., Miething, C., Dickins, R.A., Hernando, E., Krizhanovsky, V., Cordon-Cardo, C., and Lowe, S.W. (2007). Senescence and tumour clearance is triggered by p53 restoration in murine liver carcinomas. *Nature* *445*, 656–660.
- Yildiz, G., Arslan-Ergul, A., Bagislar, S., Konu, O., Yuzugullu, H., Gursoy-Yuzugullu, O., Ozturk, N., Ozen, C., Ozdag, H., Erdal, E., et al. (2013). Genome-wide transcriptional reorganization associated with senescence-to-immortality switch during human hepatocellular carcinogenesis. *PLoS One* *8*, e64016.
- Yuzefpolskiy, Y., Baumann, F.M., Kalia, V., and Sarkar, S. (2015). Early CD8 T-cell memory precursors and terminal effectors exhibit equipotent in vivo degranulation. *Cell Mol. Immunol.* *12*, 400–408.
- Zigmond, E., Samia-Grinberg, S., Pasmank-Chor, M., Brazowski, E., Shibolet, O., Halpern, Z., and Varol, C. (2014). Infiltrating monocyte-derived macrophages and resident Kupffer cells display different ontogeny and functions in acute liver injury. *J. Immunol.* *193*, 344–353.